



Plasma deposition of silver nanoparticles onto poly(ethylene terephthalate) surfaces for the preparation of antimicrobial materials

Hanène Salmi-Mani , Grégory Balthazar, Christophe J. Atkins, Caroline Aymes-Chodur, Patrick Ribot, Gabriel Terreros, Nadine Barroca-Aubry, Christophe Regeard, Philippe Roger

Received: 10 October 2022 / Revised: 1 December 2022 / Accepted: 6 December 2022
© American Coatings Association 2023

Abstract Poly(ethylene terephthalate) (PET) films were surface-modified according to microwave plasma activation allowing for dithiol functions grafting (1,6-hexanedithiol) in order to fabricate self-assembled photogenerated silver nanoparticles monolayers. The present study was carried out in constant discharge power conditions and the impact of the plasma treatment on PET wettability properties were reported. PET material modifications were characterized at various stages of the process: plasma activation, dithiol functionalization, and nanosilver grafting according to several experimental techniques: water contact angle measurements and X-ray photoelectron spectroscopy (XPS). The surface topography was studied by atomic force microscopy (AFM). Finally, antibacterial properties of PET material including silver nanoparticles were evaluated to determine the probability to reduce the surface bacterial adhesion of *Staphylococcus aureus* strain selected as pathogenic bacteria model. Surface grafted with silver nanoparticles was found to be particularly reactive and led to an inhibition of *S. aureus* adhesion around 96.2% in comparison with the unmodified PET material.

Keywords Highly performing antibacterial poly(ethylene terephthalate) (PET) surfaces, Microwave plasma activation, Thiol immobilization, Silver nanoparticles photogeneration, Self-assembled monolayers, Antibacterial coatings

Introduction

Due to its low cost, thermal stability, surface inertness, and excellent moisture resistance, poly(ethylene terephthalate) (PET) material constitutes one of the most commonly-used plastics in the world.^{1–3} In fact, PET plastic is frequently used in the food industry, where it is mainly employed as containers for various food and fluids, such as mineral water bottles.^{4,5} Similarly, PET constitutes one of the most common polymers used for medical fields. In fact, PET is massively used as blood compatible biomaterial because of its excellent mechanical properties, transparency, and relatively good biocompatibility.^{6–8}

For biomedical applications, potential bacterial contaminations of medical devices when the materials are implanted in the human body, resulting from the interaction between the substrate and pathogenic bacteria, constitute a life-threatening complication leading each year to significant patient mortality and morbidity.^{9,10} As a consequence, over the last few years, an important number of studies have reported new strategies for the enhancement of antibacterial properties of polymer according to surface modification procedures.^{11–15}

In fact, literature reported three major strategies for the development of surfaces with antibacterial activities: 1) bacteriostatic surfaces with the ability to inhibit the bacterial growth; (2) antiadhesive surfaces through the reduction in the adhesion between bacteria and the surface; and (3) bactericidal or biocide surfaces able to kill attached bacteria on the surface.

H. Salmi-Mani (✉), G. Balthazar, C. Aymes-Chodur, P. Ribot, N. Barroca-Aubry, P. Roger
Institut de Chimie Moléculaire et des Matériaux d'Orsay (ICMMO), Equipe Synthèse de Molécules et de Macromolécules pour le Vivant et l'Environnement (SM2ViE), CNRS UMR 8182, Université Paris-Saclay, 91405 Orsay Cedex, France
e-mail: hanene.salmi@universite-paris-saclay.fr

C. J. Atkins
University of Warwick, Coventry CV4 7AL, UK

G. Terreros, C. Regeard
Institute for Integrative Biology of the Cell (I2BC), CEA, CNRS, Université Paris-Saclay, 91198 Gif-sur-Yvette Cedex, France

Plasma treatment has been shown to be an extremely attractive method to modify the surface properties of polymeric materials through surface functionalization, ensuring the development of antibacterial materials.^{16–18}

An easy technique to give highly effective antibacterial properties to material consists in the immobilization of biocide species, such as silver nanoparticles, on the surface of the considered material.^{19–26} Indeed, silver nanoparticles have found numerous applications in biological, medical or pharmaceutical fields.^{27–30} Currently, nanosilver particles are considered as an alternative to classical antibiotics developed by pharmaceutical companies against Gram-positive and Gram-negative pathogenic bacteria and seem to have a high potential to solve the problem of the emergence of bacterial multidrug resistance.^{31–34} The antimicrobial mechanism of silver nanoparticles is not yet clearly understood; literature suggests a combination of multiple effects on microorganisms. Silver nanoparticles would affect the mitochondrial respiratory chain, causing ROS generation and affecting the production of ATP, which subsequently leads to DNA damage, resulting in cell death.³⁵

The present paper concerns the development of PET material presenting antibacterial activity. Thus, in order to give antibacterial properties to PET substrates, material is activated through microwave plasma discharge pretreatment and subsequently grafted with dithiol components (1,6-hexanedithiol) to introduce reactive thiol species on surface. The second step consists in the immobilization of nanosilver particles according to a UV sustainable process to fabricate robust self-assembled monolayers of thiol/biocide nanosilver material for antibacterial goals.

Effect of the plasma treatment on the wettability characteristics of the activated material is studied according to several experimental techniques. The composition and chemical structure of PET substrate and its change with surface modifications are examined by X-ray photoelectron spectroscopy (XPS), while water contact angle measurements study the change in hydrophilicity. Additionally, the surface roughness of the plasma treated films is evaluated by atomic force microscopy measurements (AFM).

Staphylococcus aureus has been selected as pathogenic bacteria model to evaluate antibacterial properties of PET material immobilized with silver nanoparticles to reduce surface bacterial adhesion. In fact, *Staphylococcus aureus* constitutes one of the major causes of bacterial contamination and transmission of health care associated infections acquired in hospital. Thereby, *Staphylococcus aureus* microorganisms cause a large range of infections from mild, such as skin infections and food poisoning, to life-threatening, such as pneumonia, sepsis, osteomyelitis, and infectious endocarditis.³⁶ This class of pathogens is particularly dangerous because it produces important toxins causing unique disease entities such as toxic-shock syndrome and staphylococcal scarlet fever, and has acquired resistance to practically

all classical antibiotics.^{37,38} In this way bacterial adhesion of *Staphylococcus aureus* on modified PET material is evaluated and compared with the activity of the untreated PET material.

Experimental part

General materials

Bi-orientated PET films Melinex OD with a thickness of 125 μm were kindly provided by DuPont Teijin films (Fig. 1). PET films were cut into pieces of $1 \times 2 \text{ cm}^2$. 1,6-Hexanedithiol (HDT, 96.0%, Fig. 1), AgNO_3 (> 99.0%), *N*-methyldiethanolamine (MDEA, $\geq 99\%$, Fig. 1), anthraquinone (AQ, 97.0%, Fig. 1), ethyl acetate (99.8%), petroleum ether (35–60 °C), dry dichloromethane, and acetonitrile (99.8%) were purchased from Aldrich and used without any purification. Water purified with a Milli-Q system (Millipore) was used for all experiments. The principal products used in the present work are represented in Fig. 1.

PET-plasma modification and thiol functionalization

Bi-oriented PET was modified using microwave argon/oxygen discharge plasma at a discharge power of 800 W during 30 s. All modified films were treated at constant discharge power and treatment time conditions. PET materials treated with microwave plasma are immediately dipped overnight in solution of 1,6-hexanedithiol (HDT) in methanol (10^{-3} M). Then, films were removed from the HDT solution and massively washed three times on methanol baths to remove HDT residual. Finally, films were dried under vacuum overnight at room temperature.

In situ photogeneration of silver nanoparticles

Thiolated films were immersed for 2 h in a mixing solution of acetonitrile containing anthraquinone (AQ, 10^{-4} M), AgNO_3 ($6 \times 10^{-2} \text{ M}$), and MDEA ($6 \times 10^{-2} \text{ M}$). Then, films were removed from the AgNO_3 solution and irradiated with an intensity of 7 mW cm^{-2} for 15 s. After irradiation, films were intensively rinsed with acetonitrile and methanol, and dried under vacuum overnight.

Antibacterial activity assessment

Gram-positive strain used in this study was *Staphylococcus aureus* (CIP4.83, Pasteur Institute Collection). Bacterial strains were stored in glycerol 15% at $-80 \text{ }^\circ\text{C}$. Adhesion tests were performed with cells in the early stationary growth phase, $\text{DO}_{580\text{nm}}$ of 1.5

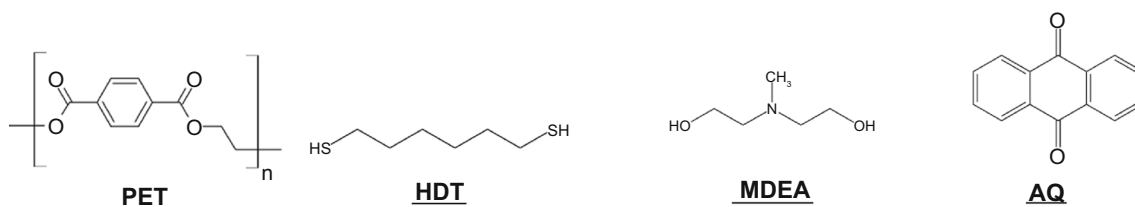


Fig. 1: Materials used in the study

(approximately 10^9 Colony Forming Unit per mL [$\text{CFU}\cdot\text{mL}^{-1}$]). Strains were cultivated in LB medium (Lennox L: 1% Bacto-Tryptone, 0.5% Bacto-Yeast Extract, 1% NaCl, NaOH [3×10^{-3} M]) at 37 °C).

Bacterial adhesion tests

Bacterial adhesion tests were performed by sedimentation. Cells in early stationary phase of growth were harvested and washed three times by centrifugation at 6000 g for 10 min at 4 °C and re-suspended in a PBS buffer (137 mM NaCl, 2.7 mM KCl, 10 mM Na_2HPO_4 , 1.76 mM KH_2PO_4 , pH 7.4). Cells were adjusted to $\text{DO}_{600\text{nm}} = 0.8$ and concentration was verified by enumeration of cultivable cell on LB plates (LB with agar 15%). Ten milliliters of cell suspension were allowed to adhere for 3 h at 37 °C for *Staphylococcus aureus* to substrate samples, modified PET-surfaces, and untreated PET-surfaces as controls in 55 mm in diameter Petri dishes. After 3 h, nonadherent or weakly attached cells were removed by six successive rinsing of substrate samples in PBS. Adherent cells were detached by ultrasonic treatment on ice for 17.5 s at 33% duty cycle and maximum output (4) using a microprobe on a Branson model 450. These parameters were previously established³⁹ and used for environmental samples.⁴⁰ The number of viable and cultivable bacteria was determined by enumeration of cultivable cell on LB plates. Each experiment was conducted three times. The percentage of bacterial adhesion inhibition was estimated by the comparison of the CFU obtained in modified PET-surfaces with untreated PET-surfaces (considered as 100%) and calculated as follows:

$$\%_{\text{bacterial adhesion}} = 100 - \frac{\text{CFU}_{\text{Untreated PET}} - \text{CFU}_{\text{Modified PET}}}{\text{CFU}_{\text{Untreated PET}}} \times 100$$

Equipment and characterization

Plasma reactor

The experimental apparatus consists of a 3 cm diameter and 90 cm high quartz cylinder fixed on top of a post-

discharge chamber (stainless steel cylinder, 5 cm diameter, 30 cm height). This reactor has been described earlier.⁴¹ In the post-discharge chamber, the substrate holder was fixed 1 cm from the end of the quartz cylinder. The plasma was generated using a Surfaguide reactor excitatory fed from opposite sides by two microwave (MW) sources at 2.45 GHz. The argon and oxygen flux were controlled by mass flow meters. Experimental conditions were the following: pressure fixed at 6×10^{-2} mBar, argon flux regulated at 500 scc/min and O_2 flux at 200 scc/min; generator was set at power of 800 W. Films were exposed to plasma for 30 s.

UV irradiation

Silver nanoparticles photogeneration was achieved using UVA Cube 100 apparatus (Dr Hönle, Hg lamp, 15 s, 7.0 mW cm^{-2} , München, Germany).

Contact angle measurements

Contact angle measurements were carried out by the Young–Laplace method using a DS100 Krüss goniometer with high purity water (Millipore, milli-Q). Water contact angle was measured within 10 s of placing the drop (3 μL) on the surface, an average of three measurements per surface was reported.

Atomic force microscopy (AFM) measurements

Atomic force microscopy measurements were conducted by tapping mode topography and phase imaging using di Innova AFM (Brüker) with NanoDrive v8.02 software. Tapping mode images were acquired using silicon tips from Nanosensors (PPPNCSTR) with a resonance frequency ranging between 76 and 263 kHz. Image processing was performed using WSxM software.⁴² RMS indicates root-mean-square roughness of obtained at focusing window of $2 \mu\text{m} \times 2 \mu\text{m}$.

X-ray photoelectron spectroscopy (XPS) measurements

X-ray photoelectron spectroscopy (XPS) measurements were performed on a K-Alpha spectrometer

from ThermoFisher, equipped with a monochromated X-ray Source (Al K α , 1486.6 eV). For all measurements, a spot size of 400 μ m was employed. The hemispherical analyzer was operated in CAE (Constant Analyzer Energy) mode, with pass energy of 200 eV and a step of 1 eV for the acquisition of surveys spectra, and pass energy of 50 eV and a step of 0.1 eV for the acquisition of high resolution spectra. A “dual beam” flood gun was used to neutralize the charge build-up. Spectra obtained were treated by means of the “Avantage” software provided by ThermoFisher. A Shirley type background subtraction was used and the peak areas were normalized using the Scofield sensitivity factors in the calculation of elemental compositions. All binding energies were referenced to C1s neutral carbon peak at 284.8 eV.

Results and discussion

The present work was focused on the development of PET material with antibacterial activity. Antimicrobial properties of the elaborated coatings were given by the immobilization of biocide silver nanoparticles onto PET surface. Silver nanoparticles immobilization was achieved by chemically modifying PET surface by a preliminary microwave plasma treatment in order to enhance the surface adhesion performances (STEP 1, Scheme 1). Plasma treatment was followed by an immediate dipping of the reactive film on a solution of 1,6-hexanedithiol solution in methanol (STEP 2, Scheme 1), in order to provide thiol groups covalently linked to the substrate. Finally, silver nanoparticles were simultaneously photogenerated and self-assembled with thiol species covering PET surface (STEP 3, Scheme 1).

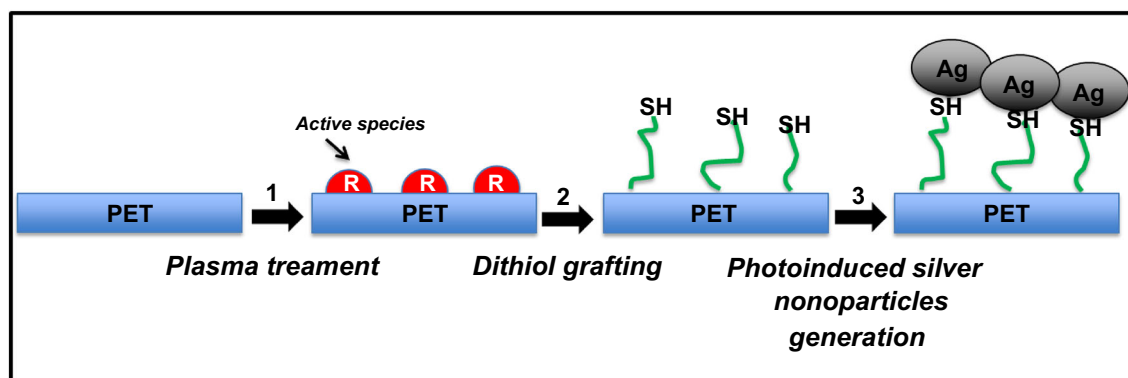
Preliminary study: effect of plasma treatment

Plasma treatment was used to improve the wettability of the PET material. O₂/Ar plasma treatment process was achieved by placing PET film in the microwave

generated plasma chamber and bombarded with ionized gas in a vacuum environment. Water contact angle measurements were performed at surface of the activated PET film, in order to characterize the efficiency of the applied plasma treatment. Figure 2 presents the variation of the water contact angles with time after 30 s of plasma treatment. All contact angle measurements were compared with the untreated PET material film.

Untreated PET material presents a relatively hydrophobic character with an associated water contact angle around 80° (Fig. 2). Subsequently to plasma treatment, more specifically immediately after plasma process, PET water contact angle value drastically decreases (Fig. 2). Thus, hydrophilicity of PET surface is improved by plasma treatment, which confirms the suitability of plasma conditions selected. By monitoring water contact angle variation with time following plasma treatment, it can be observed that hydrophilicity character of the activated PET surface decreases with time. Measured only 30 min after plasma process, PET water contact angle increases again around 70° (Fig. 2), getting closer to initial PET value (80°, Fig. 2). The improvement of the hydrophilicity of the surface through the plasma treatment is the consequence of the generation of hydrophilic functional groups (C–O, C=O, (C=O)–O, etc.), and other reactive ions and electrons.^{43–45} This phenomenon is clearly visualized in Table 1 describing the elemental composition of untreated PET versus plasma treated PET (PET-plasma). In fact, plasma process leads to an increase in the oxygen elemental concentration determined by XPS analysis. In comparison with the untreated PET substrate, a higher O/C elemental surface concentration ratio is observed (0.49 *versus* 0.38, respectively, for the PET–plasma and the untreated PET) which is correlated with the production of hydrophilic species on the top of the surface through plasma treatment. Unfortunately, at long term, the hydrophilicity of the activated surface fades due to recombination process of radical species and electron-ions (Fig. 2).

These results suggest that the best wettability performances are obtained immediately after plasma



Scheme 1: Strategy employed for the immobilization of silver nanoparticles onto PET-surfaces

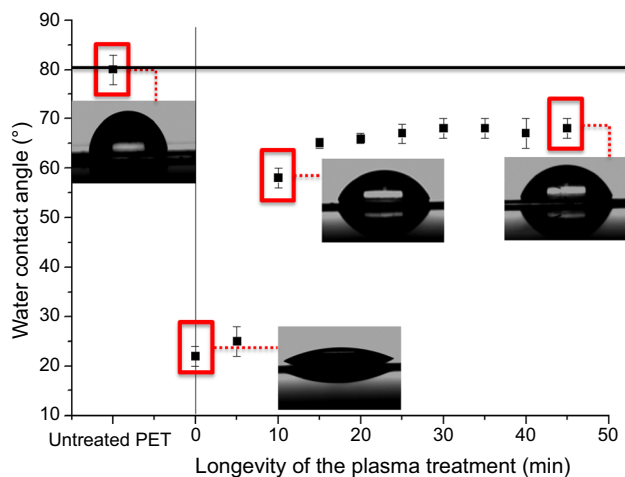


Fig. 2: Water contact angles variation with time after plasma treatment (plasma conditions: gas O_2/Ar , 800 W, 30 s)

Table 1: Elemental composition (%) of untreated PET, PET-plasma, PET-plasma-SH, and PET-plasma-SH-Ag substrates

Sample	C (1s)	O (1s)	S (2p)	Ag (3d)
Untreated PET	72.0	28.0	–	–
PET-plasma	67.0	33.0	–	–
PET-plasma-SH	70.4	28.9	0.7	–
PET-plasma-SH-Ag	71.5	27.5	0.3	0.7

process. Thus these operating conditions were chosen for the grafting of thiol species (HDT) followed by silver nanoparticles immobilization onto PET substrate.

Thiol grafting on plasma treated PET

Plasma treatment leads to a hydrophilic surface suitable for thiol binding. Immediately after plasma treatment, activated PET film is dipped in a solution of 1,6-hexanedithiol (HDT) in methanol. After film washing and drying under vacuum, water contact angle was measured. Thiol grafting leads to an increase in the associated water contact angle value, while maintaining a hydrophilic behavior to the surface (Table 2). In fact, water contact angle increases from 23° for the plasma treated PET surface to 46° for the same PET film grafted with thiol functions (PET-plasma-SH). Similar results have been reported for the grafting of cysteamine through plasma treated PET-surfaces.⁴⁶ This result reflects a combination of two effects: the aging of the plasma treated surface due to a rearrangement of created polar groups onto PET surface combined with the grafting of hydrophilic thiol groups from HDT moiety.

Surface topography and roughness may play an important role on the process of thiol grafting. Thus, roughness and morphology of untreated PET, PET-plasma treated, and PET-plasma-SH substrates were examined by AFM technique (Fig. 3).

Untreated PET surface is relatively smooth with a root-mean-square (RMS) roughness around 1.7 nm (untreated PET, Fig. 3a) with some defects due to the manufacturing. After plasma treatment, PET substrates becomes rougher with a RMS value of 3.1 nm due to abrasive plasma process allowing to adhesion properties enhancement. Subsequently, through the dipping of the previous plasma treated film in HDT solution, a reinforcement of the surface roughness (RMS = 9.5 nm, Fig. 3c) is observed. Based on these results, it can be concluded that both, plasma treatment and HDT grafting, have an important impact on the surface roughness and morphology of treated PET-surfaces.

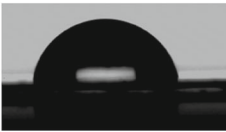
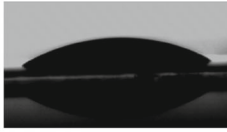
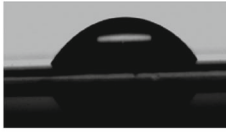
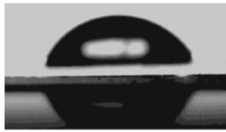
To confirm the success of grafting of HDT molecules onto PET-plasma surface, XPS measurements were carried out; the results are shown on Fig. 4 and Table 1.

Subsequently to plasma treatment, a signal at binding energy value around 168 eV corresponding to sulfur S2p contribution is clearly observed in the XPS survey (Fig. 4a) with an atomic ratio around 0.7% (Table 1). S2p signal associated to PET-plasma-SH (Fig. 4b) shows a doublet centered at 163 eV and 168 eV. First peak corresponds to the presence of a S–C and S–H bonds,⁴⁷ while peak at higher binding energy corresponds to S–O bonds⁴⁸ confirming the HDT grafting on the plasma activated PET surface.

Silver nanoparticles immobilization

Surface anchoring thiol species can constitute an effective platform for silver nanoparticles immobilization via Ag–S bond formation.⁴⁹ Only few studies describe nanosilver immobilization onto organic polymer surfaces.^{50–52} Actually, literature classically reports the attachment of silver nanoparticles on various inorganic surfaces.^{53,54} In the present work, thiols grafted on PET surface are employed to covalently link silver nanoparticles simultaneously generated according to a photoinduced reduction process. Photoinduced reduction method presents several advantages in terms of green technique requiring low energy, no excess of reducing agent or solvent, combined with a control of the morphology and size of the generated nanoparticles.^{55,56} To this end, PET-plasma-SH substrates are incubated in a solution of $AgNO_3$ /MDEA (reducing agent)/AQ (photosensitizer) in acetonitrile, then briefly UV irradiated. In comparison with the only plasma treated PET, water contact angle measured after nanosilver immobilization shows an enhancement of the hydrophobic behavior of the film with a value around 69° (Table 2). Similar results have been described for immobilization of silver nanoparticles

Table 2: Water contact angles after each step of the treatment: (a) Untreated PET, (b) PET-plasma, (c) PET-plasma-SH, and (d) PET-plasma-SH-Ag

(a)	(b)	(c)	(d)
			
80°±2	23°±3	46°±1	69°±3

on polysulfone ultra filtration membrane via poly-dopamine (PDA) deposition and in situ reduction in silver ammonia aqueous solution.⁵⁷ This result may be partly due to a rough surface of PET-plasma-SH-Ag film, as confirmed by the observation of the surface AFM images associated to the film. Indeed, the existence of some small granular-type structures that may reveal the deposition of silver nanoparticles, is observed on the film (Fig. 3d) combined with an increasing of the surface roughness with a RMS value of 15.3 nm.

XPS analysis clearly confirms the immobilization of silver nanoparticles onto PET surface with the apparition of silver atoms in the XPS survey (binding energies of Ag3d_{5/2} and Ag3d_{3/2} at 374 eV and 368 eV, respectively). The splitting of the 3d doublet of Ag is about 6.0 eV, proving the formation of metallic Ag NP (Ag⁰) with an atomic ratio around 0.7% (Fig. 4c and Table 1) onto PET surface.^{58,59}

Antibacterial activity

Literature reports that silver nanoparticles constitute a nonspecific antibacterial agent against a wide range of pathogenic microorganisms.^{31,33,60–62} *Staphylococcus aureus* belongs to the Gram-positive bacterium grouped with *Bacillus Subtilis* on the basis of ribosomal RNA sequences.³⁷ Figure 4 presents the antibacterial activities associated with PET-plasma-SH and PET-plasma-SH-Ag substrates compared to the untreated PET acting as control experiment.

Interestingly, in comparison with the untreated PET material, antibacterial tests evaluated against *Staphylococcus aureus* (CIP4.83, Pasteur Institute Collection) exhibit a greater cell attachment through thiol grafting (PET-plasma-SH, Fig. 5). The initial number of bacterial cells was 1.8×10^6 CFU/cm² (untreated PET, Fig. 5a) and a number of resultant colonies counted after 3 h of incubation increased with a concentration of 2.2×10^6 CFU/cm² corresponding to an increasing of the bacterial adhesion around 20% (Fig. 5b). Similar

results have been reported for hyper branched thiol-functionalized stainless steel substrates.⁶³ It has been demonstrated that free thiol groups positively affect cell behavior via enhancing the surface potential of the scaffolds and providing additional adhesion sites for the cells.^{64–66}

On the other hand, surface roughness could constitute also an important factor influencing bacterial adhesion. In fact, subsequently to thiol grafting an increasing of the surface roughness is observed (Fig. 4 c). It is well known that the irregularities of polymeric surfaces promote bacterial adhesion, rough surfaces have a greater surface area and the depressions in the roughened surface provide more favorable sites for bacterial colonization.⁴⁴

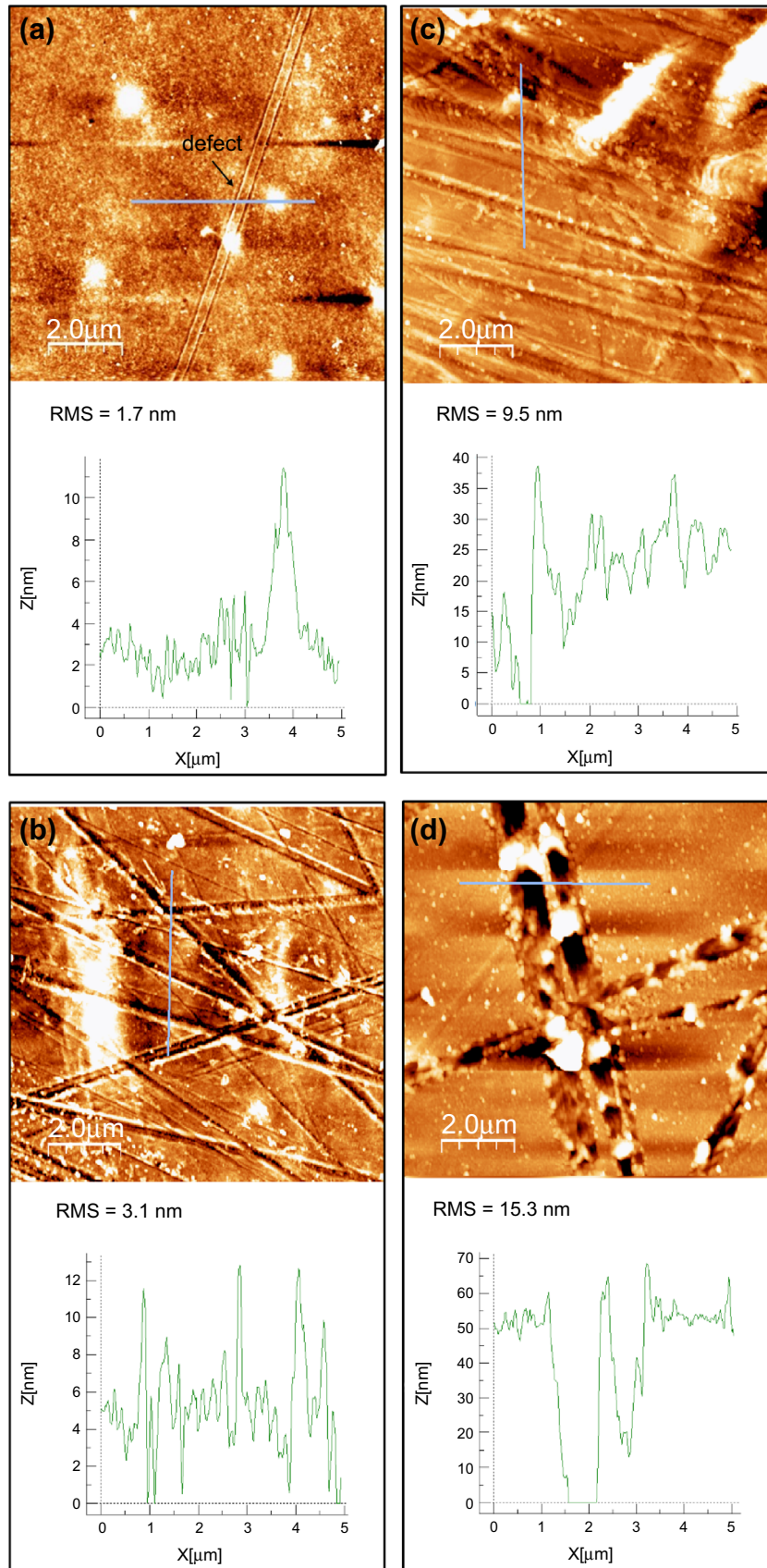
The introduction of silver nanoparticles into PET-based material leads to a drastic inhibition of the bacterial adhesion against *Staphylococcus aureus* strain. Indeed, PET-plasma-SH-Ag material presents a residual bacterial adhesion of 3.8% (7.0×10^4 CFU/cm²) (Fig. 5b) compared to untreated PET material.

These results clearly indicate that the incorporation of silver nanoparticles onto PET-plasma-SH platform constitutes an efficient method for substantially enhancing the antibacterial activity of classical PET material, and thus preventing the proliferation of bacteria on material surfaces.

Conclusions

PET substrates were successfully modified by O₂/Ar microwave plasma discharge to activate polymer material in order to ensure the anchoring of reactive thiol functions onto PET surface. Thus, thiol coating has been efficiently used to immobilize silver nanoparticles according to an in situ photoinduced process.

Lastly, PET material incorporated with nanosilver showed significant inhibition of adhesion against *Staphylococcus aureus* compared to unmodified PET substrate. In fact, in comparison with the untreated PET, hybrid PET material exhibited an inhibition of



◀Fig. 3: AFM topographic images and corresponding cross sections associated to: a Untreated PET, b PET-plasma, c PET-plasma-SH, and d PET-plasma-SH-Ag substrates. Value of the surface root-mean-square (RMS) roughness is presented for all samples

adhesion against *Staphylococcus aureus* around 96.2%. This inhibition results from two combined effects, the highly biocide performances of nanosilver species associated with developing a rough PET surface which is inappropriate for bacterial adhesion.

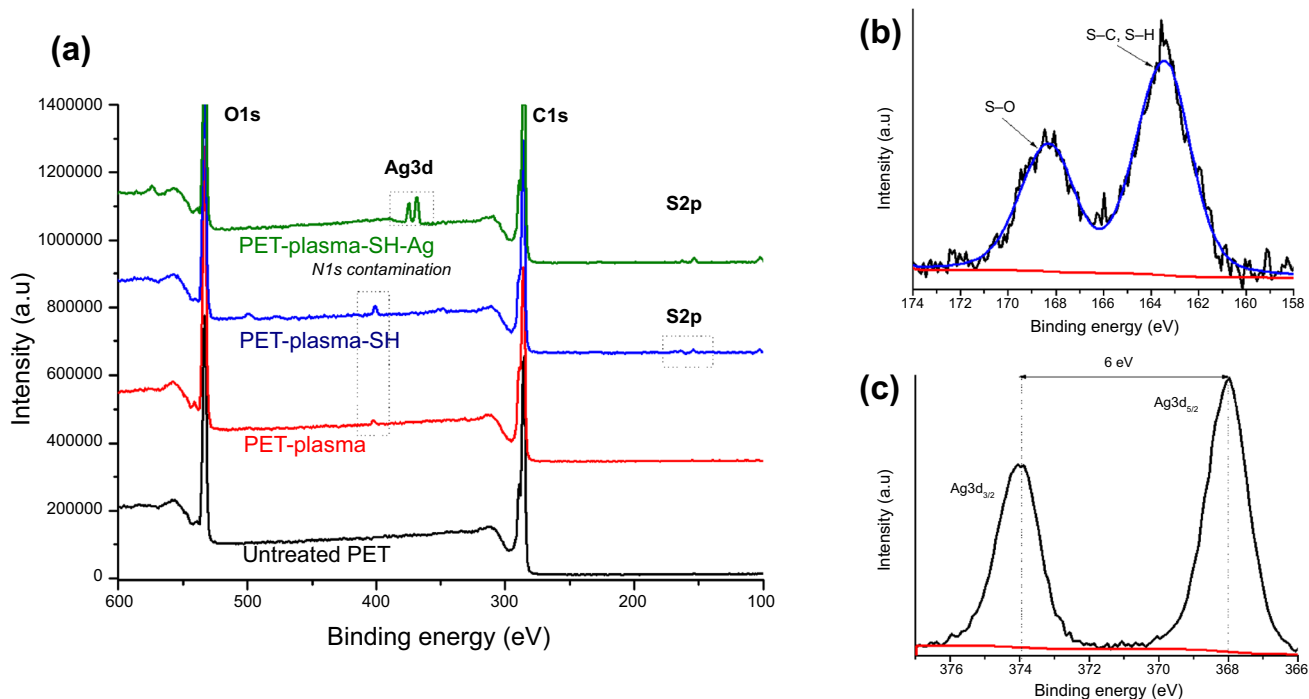


Fig. 4: a XPS survey of untreated PET, PET-plasma, PET-plasma-SH, and PET-plasma-SH-Ag substrates; b XPS spectra of S2p core-level of PET-plasma-SH; c XPS spectra of Ag3d core-level PET-plasma-SH-Ag PET sample. A small N1s peak at 400 eV, assigned to an adventitious contamination during XPS experiments, was observed

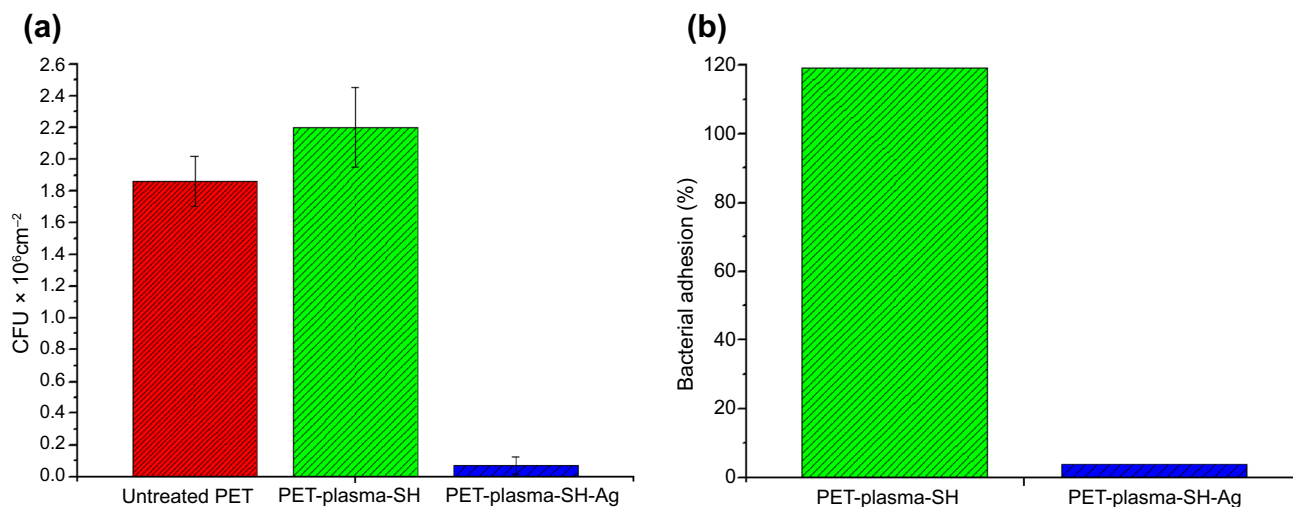


Fig. 5: a Comparison of antiadhesive activity against *Staphylococcus aureus* of untreated PET, PET-plasma-SH, and PET-plasma-SH-Ag substrates; b Percentage of resulting bacterial adhesion of PET-plasma-SH and PET-plasma-SH-Ag materials against *Staphylococcus aureus* compared to untreated PET acting as control experiment

Finally, the strategy presented in this work constitutes an easy and environmentally friendly approach to prepare polyester polymers with antibacterial activities for biomedical or biological applications, to solve the problems of bacterial contaminations.

References

- Barber, NA, *Polyethylene Terephthalate: Uses Properties and Degradation*. Nova Science Publishers, Hauppauge (2017)
- Visakh, PM, Liang, M, *Poly(ethylene terephthalate) Based Blends Composites and Nanocomposites*. William Andrew, Norwich (2015)
- Thomas, S, Visakh, PM, *Handbook of Engineering and Specialty Thermoplastics: Polyethers and Polyesters*. Wiley, Hoboken (2011)
- Bach, C, Dauchy, X, Chagnon, M-C, Etienne, S, “Chemical Compounds and Toxicological Assessments of Drinking Water Stored in Polyethylene Terephthalate (PET) Bottles: A Source of Controversy Reviewed.” *Water Res.*, **46** 571–583. <https://doi.org/10.1016/j.watres.2011.11.062> (2012)
- Lange, J, Wyser, Y, “Recent Innovations in Barrier Technologies for Plastic Packaging? A Review.” *Packag. Technol. Sci.*, **16** 149–158. <https://doi.org/10.1002/pts.621> (2003)
- Kim, YJ, Kang, I-K, Huh, MW, Yoon, S-C, “Surface Characterization and In Vitro Blood Compatibility of Poly(ethylene terephthalate) Immobilized with Insulin and/or Heparin Using Plasma Glow Discharge.” *Biomaterials*, **21** 121–130. [https://doi.org/10.1016/S0142-9612\(99\)00137-4](https://doi.org/10.1016/S0142-9612(99)00137-4) (2000)
- Wang, J, Pan, CJ, Huang, N, Sun, H, Yang, P, Leng, YX, Chen, JY, Wan, GJ, Chu, PK, “Surface Characterization and Blood Compatibility of Poly(ethylene terephthalate) Modified by Plasma Surface Grafting.” *Surf. Coat. Technol.*, **196** 307–311. <https://doi.org/10.1016/j.surfcoat.2004.08.161> (2005)
- Ueda, T, Oshida, H, Kurita, K, Ishihara, K, Nakabayashi, N, “Preparation of 2-Methacryloyloxyethyl Phosphorylcholine Copolymers with Alkyl Methacrylates and Their Blood Compatibility.” *Polym. J.*, **24** 1259–1269. <https://doi.org/10.1295/polymj.24.1259> (1992)
- Stamm, WE, “Infections Related to Medical Devices.” *Ann. Int. Med.*, **89** 764–769. <https://doi.org/10.7326/0003-4819-89-5-764> (1978)
- von Eiff, C, Jansen, B, Kohnen, W, Becker, K, “Infections Associated with Medical Devices.” *Drugs*, **65** 179–214. <http://doi.org/10.2165/00003495-200565020-00003> (2005)
- Raad, II, Darouiche, RO, “Antibacterial Coated Medical Implants.” <https://patents.google.com/patent/US5217493A/en> (1993)
- Vasilev, K, Cook, J, Griesser, HJ, “Antibacterial Surfaces for Biomedical Devices.” *Expert Rev. Med. Devices*, **6** 553–567. <https://doi.org/10.1586/erd.09.36> (2009)
- Qiu, H, Si, Z, Luo, Y, Feng, P, Wu, X, Hou, W, Zhu, Y, Chan-Park, MB, Xu, L, Huang, D, “The Mechanisms and the Applications of Antibacterial Polymers in Surface Modification on Medical Devices.” *Front. Bioeng. Biotechnol.*, **8** 910. <https://doi.org/10.3389/fbioe.2020.00910> (2020)
- Dixit, A, Wazarkar, K, Sabnis, AS, “Antimicrobial UV Curable Wood Coatings Based on Citric Acid.” *Pigm. Resin Technol.*, **50** 533–544. <https://doi.org/10.1108/PRT-07-2020-067> (2021)
- Dixit, A, Sabnis, A, Shetty, A, “Antimicrobial Edible Films and Coatings based on N, O-Carboxymethyl Chitosan Incorporated with Ferula Asafoetida (Hing) and Adhatoda Vasica (Adulsa) Extract.” *Adv. Mater. Process. Technol.* <https://doi.org/10.1080/2374068X.2021.1939982> (2021)
- Huh, MW, Kang, I-K, Lee, DH, Kim, WS, Lee, DH, Park, LS, Min, KE, Seo, KH, “Surface Characterization and Antibacterial Activity Of Chitosan-Grafted Poly(ethylene terephthalate) Prepared by Plasma Glow Discharge.” *J. Appl. Polym. Sci.*, **81** 2769–2778. <https://doi.org/10.1002/app.1723> (2001)
- Jacobs, T, Morent, R, De Geyter, N, Dubruel, P, Leys, C, “Plasma Surface Modification of Biomedical Polymers: Influence on Cell-Material Interaction.” *Plasma Chem. Plasma Process.*, **32** 1039–1073. <https://doi.org/10.1007/s11090-012-9394-8> (2012)
- Špitalský, Z, Rástočná Illová, D, Žigo, O, Mičušík, M, Nógellová, Z, Procházka, M, Kleinová, A, Kováčová, M, Novák, I, “Assessment of the Antibacterial Behavior of Polyester Fabric Pre-treated with Atmospheric Discharge Plasma.” *Fibers Polym.*, **20** 1649–1657. <https://doi.org/10.1007/s12221-019-1127-7> (2019)
- Agnihotri, S, Mukherji, S, Mukherji, S, “Antimicrobial Chitosan–PVA Hydrogel as a Nanoreactor and Immobilizing Matrix for Silver Nanoparticles.” *Appl. Nanosci.*, **2** 179–188. <https://doi.org/10.1007/s13204-012-0080-1> (2012)
- Liao, Y, Wang, Y, Feng, X, Wang, W, Xu, F, Zhang, L, “Antibacterial Surfaces Through Dopamine Functionalization and Silver Nanoparticle Immobilization.” *Mater. Chem. Phys.*, **121** 534–540. <https://doi.org/10.1016/j.matchemphys.2010.02.019> (2010)
- Lin, J-J, Lin, W-C, Li, S-D, Lin, C-Y, Hsu, S, “Evaluation of the Antibacterial Activity and Biocompatibility for Silver Nanoparticles Immobilized on Nano Silicate Platelets.” *ACS Appl. Mater. Interfaces*, **5** 433–443. <https://doi.org/10.1021/a302534k> (2013)
- Vasil'kov, A, Budnikov, A, Gromovych, T, Pigaleva, M, Sadykova, V, Arkharova, N, Naumkin, A, “Effect of Bacterial Cellulose Plasma Treatment on the Biological Activity of Ag Nanoparticles Deposited Using Magnetron Deposition.” *Polymers*, **14** 3907. <https://doi.org/10.3390/polym14183907> (2022)
- Ribeiro, AI, Mehraani, B, Magalhães, C, Nicolau, T, Melro, L, Fernandes, RDV, Shvalya, V, Cvelbar, U, Padrão, J, Zille, A, “Enhancing the Antimicrobial Efficacy of Polyester Fabric Impregnated with Silver Nanoparticles Using DBD Plasma Treatment.” *Mater. Sci. Forum*, **1063** 91–97. <https://doi.org/10.4028/p-256i32> (2022)
- Hurtuková, K, Fajstavrová, K, Rimpelová, S, Vokatá, B, Fajstavr, D, Kasálková, NS, Siegel, J, Svorčík, V, Slepíčka, P, “Antibacterial Properties of a Honeycomb-like Pattern with Cellulose Acetate and Silver Nanoparticles.” *Materials*, **14** 4051. <https://doi.org/10.3390/ma14144051> (2021)
- Malapit, GM, Baculi, RQ, “Bactericidal Efficiency of Silver Nanoparticles Deposited on Polyester Fabric Using Atmospheric Pressure Plasma Jet System.” *J. Text. Inst.*, **113** 1878–1886. <https://doi.org/10.1080/00405000.2021.1954426> (2022)
- Baculi, RQ, Malapit, GM, Abayao, LE, “Atmospheric Pressure Plasma Deposition of Silver Nanoparticles on Bark Fabric for Bacterial Growth Inhibition.” *J. Textile Inst.*, <https://doi.org/10.1080/00405000.2021.2024378> (2022)
- Haider, A, Kang, I-K, “Preparation of Silver Nanoparticles and Their Industrial and Biomedical Applications: A Comprehensive Review.” *Adv. Mater. Sci. Eng.*, **2015** 1–16. <http://doi.org/10.1155/2015/165257> (2015)
- Burdusel, A-C, Gherasim, O, Grumezescu, AM, Mogoantă, L, Ficai, A, Andronescu, E, “Biomedical Applications of

- Silver Nanoparticles: An Up-to-Date Overview.” *Nanomaterials*, **8** 681. <https://doi.org/10.3390/nano8090681> (2018)
29. García-Barrasa, J, López-de-Luzuriaga, J, Monge, M, “Silver Nanoparticles: Synthesis Through Chemical Methods in Solution and Biomedical Applications.” *Open Chem.*, **9** 7–19. <https://doi.org/10.2478/s11532-010-0124-x> (2011)
 30. Mathur, P, Jha, S, Ramteke, S, Jain, NK, “Pharmaceutical Aspects of Silver Nanoparticles.” *Artif. Cells, Nanomed. Biotechnol.*, **46** 115–126. <https://doi.org/10.1080/21691401.2017.1414825> (2018)
 31. Rai, MK, Deshmukh, SD, Ingle, AP, Gade, AK, “Silver Nanoparticles: The Powerful Nanoweapon Against Multidrug-Resistant Bacteria.” *J. Appl. Microbiol.*, **112** 841–852. <https://doi.org/10.1111/j.1365-2672.2012.05253.x> (2012)
 32. Rai, M, Yadav, A, Gade, A, “Silver Nanoparticles as a New Generation of Antimicrobials.” *Biotechnol. Adv.*, **27** 76–83. <https://doi.org/10.1016/j.biotechadv.2008.09.002> (2009)
 33. Franci, G, Falanga, A, Galdiero, S, Palomba, L, Rai, M, Morelli, G, Galdiero, M, “Silver Nanoparticles as Potential Antibacterial Agents.” *Molecules*, **20** 8856–8874. <https://doi.org/10.3390/molecules20058856> (2015)
 34. Mulani, MS, Kamble, EE, Kumkar, SN, Tawre, MS, Pardesi, KR, “Emerging Strategies to Combat ESKAPE Pathogens in the Era of Antimicrobial Resistance: A Review.” *Front. Microbiol.*, **10** 539. <https://doi.org/10.3389/fmicb.2019.00539> (2019)
 35. Morones, JR, Elechiguerra, JL, Camacho, A, Holt, K, Kouri, JB, Ramírez, JT, Yacaman, MJ, “The Bactericidal Effect of Silver Nanoparticles.” *Nanotechnology*, **16** 2346–2353. <https://doi.org/10.1088/0957-4484/16/10/059> (2005)
 36. Reddy, PN, Srirama, K, Dirisala, VR, “An Update on Clinical Burden, Diagnostic Tools, and Therapeutic Options of *Staphylococcus aureus*.” *Infect. Dis. (Auckl)*, **10** 1179916117703999. <https://doi.org/10.1177/1179916117703999> (2017)
 37. Kuroda, M, Ohta, T, Uchiyama, I, Baba, T, Yuzawa, H, Kobayashi, I, Cui, L, Oguchi, A, Aoki, K, Nagai, Y, Lian, J, Ito, T, Kanamori, M, Matsumaru, H, Maruyama, A, Murakami, H, Hosoyama, A, Mizutani-Ui, Y, Takahashi, NK, Sawano, T, Inoue, R, Kaito, C, Sekimizu, K, Hirakawa, H, Kuhara, S, Goto, S, Yabuzaki, J, Kanehisa, M, Yamashita, A, Oshima, K, Furuya, K, Yoshino, C, Shiba, T, Hattori, M, Ogasawara, N, Hayashi, H, Hiramatsu, K, “Whole Genome Sequencing of Meticillin-Resistant *Staphylococcus aureus*.” *Lancet*, **357** 1225–1240. [https://doi.org/10.1016/S0140-6736\(00\)04403-2](https://doi.org/10.1016/S0140-6736(00)04403-2) (2001)
 38. Mediavilla, JR, Chen, L, Mathema, B, Kreiswirth, BN, “Global Epidemiology of Community-Associated Methicillin Resistant *Staphylococcus aureus* (CA-MRSA).” *Curr. Opin. Microbiol.*, **15** 588–595. <https://doi.org/10.1016/j.mib.2012.08.003> (2012)
 39. Prigent, M, Leroy, M, Confalonieri, F, Dutertre, M, DuBow, MS, “A Diversity of Bacteriophage Forms and Genomes can be Isolated from the Surface Sands of the Sahara Desert.” *Extremophiles*, **9** 289–296. <https://doi.org/10.1007/s00792-005-0444-5> (2005)
 40. Prestel, E, Regard, C, Salamitou, S, Neveu, J, Dubow, MS, “The Bacteria and Bacteriophages from a Mesquite Flats Site of the Death Valley Desert.” *Antonie Van Leeuwenhoek*, **103** 1329–1341. <https://doi.org/10.1007/s10482-013-9914-4> (2013)
 41. Bech, L, Lepoittevin, B, El Achhab, A, Lepleux, E, Teulé-Gay, L, Boisse-Laporte, C, Roger, P, “Double Plasma Treatment-Induced Graft Polymerization of Carbohydrated Monomers on Poly(ethylene terephthalate) Fibers.” *Langmuir*, **23** 10348–10352. <https://doi.org/10.1021/la701400b> (2007)
 42. Horcas, I, Fernández, R, Gómez-Rodríguez, JM, Colchero, J, Gómez-Herrero, J, Baro, AM, “WSXM: A Software for Scanning Probe Microscopy and a Tool for Nanotechnology.” *Rev. Sci. Instrum.*, **78** 013705. <https://doi.org/10.1063/1.2432410> (2007)
 43. Fang, Z, Yang, J, Liu, Y, Shao, T, Zhang, C, “Surface Treatment of Polyethylene Terephthalate to Improving Hydrophilicity Using Atmospheric Pressure Plasma Jet.” *IEEE Trans. Plasma Sci.*, **41** 1627–1634. <https://doi.org/10.1109/TPS.2013.2259508> (2013)
 44. Švorčík, V, Řezníčková, A, Sajdl, P, Kolská, Z, Makajová, Z, Slepíčka, P, “Au Nanoparticles Grafted on Plasma Treated Polymers.” *J Mater Sci.*, **46** 7917–7922. <https://doi.org/10.1007/s10853-011-5920-y> (2011)
 45. Švorčík, V, Chaloupka, A, Záruba, K, Král, V, Bláhová, O, Macková, A, Hnatowicz, V, “Deposition of Gold Nanoparticles and Nano-Layers on Polyethylene Modified by Plasma Discharge and Chemical Treatment.” *Nucl. Instrum. Methods Phys. Res. Sect. B Beam Interactions Mater. Atoms*, **267** 2484–2488. <https://doi.org/10.1016/j.nimb.2009.05.071> (2009)
 46. Kolská, Z, Řezníčková, A, Nagyová, M, Slepíčková Kasálková, N, Sajdl, P, Slepíčka, P, Švorčík, V, “Plasma Activated Polymers Grafted with Cysteamine Improving Surfaces Cytocompatibility.” *Polym. Degrad. Stab.*, **101** 1–9. <https://doi.org/10.1016/j.polymdegradstab.2014.01.024> (2014)
 47. Castner, DG, Hinds, K, Grainger, DW, “X-ray Photoelectron Spectroscopy Sulfur 2p Study of Organic Thiol and Disulfide Binding Interactions with Gold Surfaces.” *Langmuir*, **12** 5083–5086. <https://doi.org/10.1021/la960465w> (1996)
 48. Castaño, JG, Arroyave, C, Morcillo, M, “Characterization of Atmospheric Corrosion Products of Zinc Exposed to SO₂ and NO₂ Using XPS and GIXD.” *J. Mater. Sci.*, **42** 9654–9662. <https://doi.org/10.1007/s10853-007-1964-4> (2007)
 49. Brust, M, Kiely, CJ, “Some Recent Advances in Nanostructure Preparation from Gold and Silver Particles: A Short Topical Review.” *Colloids Surf. A Physicochem. Eng. Aspects*, **202** 175–186. [https://doi.org/10.1016/S0927-7757\(01\)01087-1](https://doi.org/10.1016/S0927-7757(01)01087-1) (2002)
 50. Misra, RDK, Girase, B, Depan, D, Shah, JS, “Hybrid Nanoscale Architecture for Enhancement of Antimicrobial Activity: Immobilization of Silver Nanoparticles on Thiol-Functionalized Polymer Crystallized on Carbon Nanotubes.” *Adv. Eng. Mater.*, **14** B93–B100. <https://doi.org/10.1002/ade.201180081> (2012)
 51. Dong, X, Shannon, HD, Amirsoleimani, A, Brion, GM, Escobar, IC, “Thiol-Affinity Immobilization of Casein-Coated Silver Nanoparticles on Polymeric Membranes for Biofouling Control.” *Polymers*, **11** 2057. <https://doi.org/10.3390/polym11122057> (2019)
 52. Reznickova, A, Kolska, Z, Zaruba, K, Svorcik, V, “Grafting of Gold Nanoparticles on Polyethyleneterephthalate Using Dithiol Interlayer.” *Mater. Chem. Phys.*, **145** 484–490. <https://doi.org/10.1016/j.matchemphys.2014.03.001> (2014)
 53. Quang, DV, Lee, JE, Kim, J-K, Kim, YN, Shao, GN, Kim, HT, “A Gentle Method to Graft Thiol-Functional Groups onto Silica Gel for Adsorption of Silver Ions and Immobilization of Silver Nanoparticles.” *Powder Technol.*, **235** 221–227. <https://doi.org/10.1016/j.powtec.2012.10.015> (2013)
 54. Suzuki, H, Chiba, H, Futamata, M, “Efficient Immobilization of Silver Nanoparticles on Metal Substrates Through Various Thiol Molecules to Utilize a Gap Mode in Surface Enhanced Raman Scattering.” *Vib. Spectrosc.*, **72** 105–110. <https://doi.org/10.1016/j.vibspec.2014.03.002> (2014)

55. Malval, J-P, Jin, M, Balan, L, Schneider, R, Versace, D-L, Chaumeil, H, Defoin, A, Soppera, O, "Photoinduced Size-Controlled Generation of Silver Nanoparticles Coated with Carboxylate-Derivatized Thioxanthenes." *J. Phys. Chem. C.*, **114** 10396–10402. <https://doi.org/10.1021/jp102189u> (2010)
56. Versace, D-L, Ramier, J, Grande, D, Andaloussi, SA, Dubot, P, Hobeika, N, Malval, J-P, Lalevee, J, Renard, E, Langlois, V, "Versatile Photochemical Surface Modification of Biopolyester Microfibrous Scaffolds with Photogenerated Silver Nanoparticles for Antibacterial Activity." *Adv. Healthcare Mater.*, **2** 1008–1018. <https://doi.org/10.1002/adhm.201200269> (2013)
57. Huang, L, Zhao, S, Wang, Z, Wu, J, Wang, J, Wang, S, "In Situ Immobilization of Silver Nanoparticles for Improving Permeability, Antifouling and Anti-Bacterial Properties of Ultrafiltration Membrane." *J. Membr. Sci.*, **499** 269–281. <https://doi.org/10.1016/j.memsci.2015.10.055> (2016)
58. Liang, M, Su, R, Huang, R, Qi, W, Yu, Y, Wang, L, He, Z, "Facile In Situ Synthesis of Silver Nanoparticles on Procyanidin-Grafted Eggshell Membrane and Their Catalytic Properties." *ACS Appl. Mater. Interfaces*, **6** 4638–4649. <https://doi.org/10.1021/am500665p> (2014)
59. Zhang, P, Shao, C, Zhang, Z, Zhang, M, Mu, J, Guo, Z, Liu, Y, "In Situ Assembly of Well-Dispersed Ag Nanoparticles (AgNPs) on Electrospun Carbon Nanofibers (CNFs) for Catalytic Reduction of 4-Nitrophenol." *Nanoscale*, **3** 3357–3363. <https://doi.org/10.1039/C1NR10405E> (2011)
60. Marambio-Jones, C, Hoek, EMV, "A Review of the Antibacterial Effects of Silver Nanomaterials and Potential Implications for Human Health and the Environment." *J. Nanopart. Res.*, **12** 1531–1551. <https://doi.org/10.1007/s11051-010-9900-y> (2010)
61. Figueiredo, EP, Ribeiro, JM, Nishio, EK, Scandorieiro, S, Costa, AF, Cardozo, VF, Oliveira, AG, Durán, N, Panagio, LA, Kobayashi, R, Nakazato, G, "New Approach For Simvastatin As an Antibacterial: Synergistic Effect with Bio-Synthesized Silver Nanoparticles Against Multidrug-Resistant Bacteria." *Int. J. Nanomed.*, **14** 7975–7985. <https://doi.org/10.2147/IJN.S211756> (2019)
62. Ghodake, G, Kim, M, Sung, J-S, Shinde, S, Yang, J, Hwang, K, Kim, D-Y, "Extracellular Synthesis and Characterization of Silver Nanoparticles-Antibacterial Activity Against Multidrug-Resistant Bacterial Strains." *Nanomaterials (Basel)*, **10** 360. <https://doi.org/10.3390/nano10020360> (2020)
63. Yang, WJ, Neoh, K-G, Kang, E-T, Lay-Ming Teo, S, Rittschof, D, "Stainless Steel Surfaces with Thiol-Terminated Hyperbranched Polymers for Functionalization Via Thiol-Based Chemistry." *Polym. Chem.*, **4** 3105. <https://doi.org/10.1039/c3py00009e> (2013)
64. Hegedűs, O, Juriga, D, Sipos, E, Voniatis, C, Juhász, Á, Idrissi, A, Zrínyi, M, Varga, G, Jedlovsky-Hajdú, A, Nagy, KS, "Free Thiol Groups on Poly(Aspartamide) Based Hydrogels Facilitate Tooth-Derived Progenitor Cell Proliferation and Differentiation." *PLoS One*, **14** (12) e0226363 (2019)
65. Galli, C, Parisi, L, Elviri, L, Bianchera, A, Smerieri, A, Lagonegro, P, Lumetti, S, Manfredi, E, Bettini, R, Macaluso, GM, "Chitosan Scaffold Modified with D-(+) Raffinose and Enriched with Thiol-Modified Gelatin for Improved Osteoblast Adhesion." *Biomed. Mater.*, **11** 015004. <https://doi.org/10.1088/1748-6041/11/1/015004> (2016)
66. Mun, EA, "Adhesion of Thiolated Silica Nanoparticles to Urinary Bladder Mucosa: Effects of PEGylation, Thiol Content and Particle Size." *Int. J. Pharmaceut.*, **7** 32–38 (2016)

Publisher's Note Springer Nature remains neutral with regard to jurisdictional claims in published maps and institutional affiliations.

Springer Nature or its licensor (e.g. a society or other partner) holds exclusive rights to this article under a publishing agreement with the author(s) or other rightsholder(s); author self-archiving of the accepted manuscript version of this article is solely governed by the terms of such publishing agreement and applicable law.